



Published in final edited form as:

AJR Am J Roentgenol. ; : 1–6. doi:10.2214/AJR.18.20947.

Clinical Implementation of a Focused MRI Protocol for Hepatic Fat and Iron Quantification

B. Dustin Pooler^{1,2}, **Diego Hernando**^{1,3}, **Scott B. Reeder**^{1,3,4,5,6}

¹Department of Radiology, University of Wisconsin School of Medicine and Public Health, E3/311 Clinical Science Center, 600 Highland Ave, Madison, WI 53792-3252.

²Madison Radiologists, S.C., Madison, WI.

³Department of Medical Physics, University of Wisconsin School of Medicine and Public Health, Madison, WI.

⁴Department of Medicine, University of Wisconsin School of Medicine and Public Health, Madison, WI.

⁵Department of Emergency Medicine, University of Wisconsin School of Medicine and Public Health, Madison, WI.

⁶Department of Biomedical Engineering, University of Wisconsin School of Medicine and Public Health, Madison, WI.

Abstract

OBJECTIVE.—The purpose of this article is to describe our institutional experience with the clinical implementation of a novel focused rapid chemical shift–encoded MRI protocol specifically intended to detect and quantify hepatic steatosis and iron overload, highlighting usage statistics and issues related to cost.

CONCLUSION.—Focused MRI examinations for specific clinical indications, such as this protocol for detection and quantification of hepatic steatosis and iron overload, are feasible in a busy clinical practice and add value for patients and referring providers.

Keywords

chemical shift–encoded MRI; focused protocol; hepatic steatosis; iron overload; limited examination; liver; MRI; proton density fat fraction; R2*; rapid examination

Nonalcoholic fatty liver disease (NAFLD) is emerging as the leading cause of chronic liver disease in the United States, afflicting an estimated 100 million Americans [1], including 10% of children [2]. Closely associated with obesity and diabetes, the earliest and hallmark feature of NAFLD is intracellular accumulation of triglycerides (i.e., hepatic steatosis). Patients with hepatic steatosis are at risk of nonalcoholic steatohepatitis, the histologically more aggressive form of NAFLD that can ultimately lead to liver cirrhosis and end-stage liver disease [3, 4] and can increase the risk of hepatocellular carcinoma [5]. Even more

important, hepatic steatosis has been associated with cardiovascular disease [6] – which remains the leading cause of death in the United States [7]–although causality between the two is still unclear [8].

Abnormal accumulation of iron within the liver most commonly results from either abnormal intestinal absorption associated with hereditary hemochromatosis or multiple blood transfusions (transfusional hemosiderosis) necessary to treat underlying anemia. Abnormal accumulation of liver iron can lead to liver damage, cirrhosis, and even hepatocellular carcinoma [9, 10]. Abnormal deposition of iron in the body can also result in cardiac toxicity, delayed puberty, and pancreatic dysfunction [11]. Importantly, hepatic iron overload has also been implicated as a cofactor in the progression of NAFLD [9], although the precise role of iron in NAFLD is not well understood.

Consequently, the presence and degree of hepatic steatosis and iron overload are of great clinical interest to hepatologists, hematologists, endocrinologists, and, increasingly, primary care providers. Historically, quantification of hepatic steatosis and iron overload could be reliably performed only by direct histologic analysis of tissue from liver biopsy [12], an invasive procedure often requiring moderate sedation and associated with risks that include bleeding, hospitalization, and, rarely, death [13].

In recent years, emerging confounder-corrected chemical shift–encoded (CSE) MRI techniques have become commercially available and are now U. S. Food and Drug Administration–approved on the three major MRI vendors (GE Healthcare, Siemens Healthcare, and Philips Healthcare). Within a single short breath-hold, quantitative CSE-MRI methods can provide iron-corrected maps of proton density fat fraction (PDFF) and fat-corrected R2* maps as accurate and precise imaging biomarkers of tissue triglyceride [14] and iron [15] concentration, respectively. In many clinical situations, the presence and severity of hepatic steatosis or iron overload may be the only relevant clinical indication for MRI; consequently, these patients may not benefit from a lengthy comprehensive MRI examination, which often require 30–60 minutes of table time. This is of particular importance in children, who may require sedation for lengthy MRI examinations.

To this end, our institution developed a focused unenhanced CSE-MRI protocol that obtains PDFF and R2* map in three breath-holds, or approximately 5 minutes of table time. Furthermore, this examination is ordered and billed as a limited abdominal MRI without contrast agent to appropriately reflect the narrow scope of this examination and reduce cost. In this work, we describe our institutional experience with the clinical implementation of this abbreviated CSE-MRI protocol designed specifically for the detection and quantification of hepatic steatosis and iron overload, highlighting usage statistics and relative cost of the examination.

Description of the Rapid Fat and Iron Protocol

Our institution developed and validated a U.S. Food and Drug Administration–approved single breath-hold CSE-MRI method of simultaneous quantification of tissue triglyceride concentration and iron overload, which has been described previously [16–18]. This CSE-

MRI technique was subsequently implemented using a focused MRI protocol, hereafter referred to as the rapid fat and iron protocol.

Per institutional guidelines, appropriate indications for the rapid fat and iron protocol include patients with known or suspected iron overload, patients at elevated risk for NAFLD or other cause of hepatic steatosis, patients with elevated liver function test (LFT) values and a high pretest suspicion of hepatic steatosis, and for monitoring of patients who are known to have these conditions. As further explained in the subsequent cost estimates section, this examination is billed with a limited modifier to reduce cost; to qualify for the limited charge, patients requiring sedation are not eligible for this limited examination, and add-on sequences are not permitted. Furthermore, a specific order set for this examination was created in our electronic medical record order system (Epic Hyperspace 2017, Epic Systems).

The rapid fat and iron protocol can be completed in approximately 5 minutes of table time and consists of three separate MRI acquisitions requiring patients to hold their breath for a total of three 15-to 20-second intervals. Sequences obtained include a three-plane localizer, CSE-MRI, and axial T2-weighted single-shot fast spin-echo.

After localization, the remainder of the examination is prescribed from the three-plane localizer sequence to cover the craniocaudal extent of the liver. The CSE-MRI acquisition (Ideal IQ, GE Healthcare), acquired in a single breath-hold, provides two main quantitative maps: liver PDFF (percentage), which serves as an imaging biomarker of liver fat, and R2* (1/s), which represents the rate of decay of the MRI signal, which is linearly related to liver iron concentration [19]. The T2-weighted single-shot fast spin-echo acquisition is also performed in a single breath-hold and provides a limited anatomic survey of the liver.

All imaging was performed on clinical 1.5-T (Signa HDxt or Optima MR450w, GE Healthcare) or 3-T (Discovery MR750 or Discovery MR750w, GE Healthcare) MRI systems using 8-to 12-channel (1.5-T) or 32-channel (3-T) phased-array torso coils. Details of the protocol acquisition parameters are listed in Table 1.

Clinical Implementation of the Rapid Fat and Iron Protocol: Initial Institutional Experience

In an effort to describe and quantify our initial clinical experience with the rapid fat and iron protocol, we gathered retrospective observational data from the imaging examinations and medical records of patients at our institution undergoing the rapid fat and iron protocol from April 2014 through October 2016. This study was approved by our institutional review board and maintained full HIPAA compliance, and a waiver of informed consent was provided by the institutional review board. We collected and recorded patient demographic information (including age and sex), examination indication, examination time, and examination results (PDFF and R2*) as reported by the interpreting radiologist. These data were collated, and a basic descriptive statistical analysis was performed.

A query of our institutional records from April 2014 through September 2017 identified a total of 78 rapid fat and iron protocol MRI examinations performed on a total of 69 patients, including 46 male and 23 female patients. The mean (\pm SD) patient age at the time of MRI was 35.5 ± 24.1 years, with an age range of 7–89 years. Of the 69 patients who underwent rapid fat and iron examination, 61 patients underwent a single examination. Seven patients underwent two examinations, and a single patient underwent three examinations for the purposes of treatment monitoring.

Indications for rapid fat and iron protocol MRI included evaluation for hepatic steatosis for 31 examinations, evaluation for iron overload for 37 examinations, and evaluation of unexpected nonspecific elevated LFT values for 10 examinations. Indications for pediatric patients (defined as patients younger than 18 years; 36/78 examinations) included hepatic steatosis for 26 examinations, iron overload for one examination (a patient with Diamond-Blackfan anemia requiring regular transfusion), and elevated LFT values for nine examinations. For adult patients (defined as patients ≥ 18 years old; 42/78 examinations), indications included hepatic steatosis for five examinations, iron overload for 36 examinations, and elevated LFT values for one examination.

The mean table time for the rapid fat and iron protocol MRI examinations was 6.8 ± 3.0 minutes (range, 2–17 minutes), with a median table time of 6 minutes. For 45 of 78 (58%) examinations, the table time was 6 minutes or less. For 11 of 78 (14%) examinations, the table time was longer than 10 minutes. Fifty-nine examinations were performed on 1.5-T scanners, and 19 examinations were performed on 3-T scanners. For no patient, including children, was any form of anesthesia or sedation used.

For patients for whom the examination indication was hepatic steatosis ($n = 31$), the mean PDFF was $24.1\% \pm 11.5\%$ (normal liver PDFF, $< 5\%$ [20]), with a range of 3–50% (Fig. 1). Liver PDFF was less than 5% in only three of 31 of these examinations. For patients for whom the examination indication was iron overload ($n = 37$), the mean $R2^*$ was $107.3 \pm 141.6 \text{ s}^{-1}$ (range, 25–590 s^{-1}) for examinations performed at 1.5 T ($n = 32$; normal liver $R2^*$, $< 60 \text{ s}^{-1}$ [16]) and $196.5 \pm 169.0 \text{ s}^{-1}$ (range, 72–485 s^{-1}) for examinations performed at 3 T ($n = 5$; normal liver $R2^*$, $< 120 \text{ s}^{-1}$). $R2^*$ was abnormally high in 18 of 37 examinations performed for iron overload (Fig. 2). All patients who were imaged for nonspecific elevated LFT values ($n = 9$) had abnormally high liver PDFF (mean, $21.1\% \pm 74\%$; range, 7–32%) with normal $R2^*$ values. In total, 87% (60/69) of patients scanned had abnormally high PDFF, $R2^*$, or both.

As previously mentioned, seven patients underwent two and one patient underwent three rapid fat and iron studies for treatment monitoring of hepatic steatosis. All patients undergoing multiple examinations were pediatric patients. These studies occurred a mean of 531 ± 235 days apart. PDFF decreased by a mean of $4.3\% \pm 12.9\%$ during the follow-up interval (Fig. 3). Five patients had liver PDFF decrease during the study period, and three patients had an increase in liver PDFF.

Cost Estimates

Given the complexities of billing and reimbursement in the current American health care system, determining the true cost of any medical procedure or test can be convoluted, and a complete analysis is beyond the scope and purpose of this Clinical Perspective. Furthermore, regional variations in cost, payers, collection, and other complexities add to that challenge. Consequently, we used publicly available data from the Centers for Medicare & Medicaid Services (CMS) to examine the relative cost of the limited fat and iron protocol, compared with other approaches and modalities. Although we think that this method offers the best generalizable comparison among imaging studies, we do acknowledge that commercial charges for imaging services are often substantially higher than the CMS figures reported here, a trend typical not just for imaging services but all medical services in the United States [21].

We retrospectively reviewed hospital financial records and queried the CMS Physician Fee Schedule for billing and reimbursement data related to the rapid fat and iron protocol examination, including technical component, professional component, and relative value unit information [22]. Our institution codes and bills the rapid fat and iron protocol MRI examination as a limited MRI of the abdomen without contrast agent, including a limited modifier (Current Procedural Terminology [CPT] code 74181–52), as recommended by *Radiology Compliance Manager* [23]. Medicare payment information obtained by querying the CMS Physician Fee Schedule global pricing on September 25, 2018, is detailed in Table 2. The 74181 CPT code generates a technical component fee of \$213.12 and a professional component fee of \$74.88, for a total fee of \$288.00, which is reduced to \$144.00 when the limited (–52) modifier is applied. This represents a reduction of 67% in cost when compared with a complete MRI of the abdomen with and without contrast agent (CPT code 74183), which generates a technical component fee of \$322.92 and a professional component fee of \$112.68, for a total fee of \$435.60 [22]. We also note that the CMS Physician Fee Schedule pricing information for CT of the abdomen without IV contrast agent (CPT code 74150) and limited ultrasound of the abdomen (CPT code 76705), both of which have been evaluated as imaging tests for the evaluation of hepatic steatosis [24, 25], are also included in Table 2.

Discussion

The data gathered from our initial clinical experience show the successful clinical implementation of a rapid quantitative fat and iron CSE-MRI protocol. This examination has a clearly defined scope of indications, including clinical suspicion of or treatment monitoring for hepatic steatosis or hepatic iron overload, and offers a relatively inexpensive alternative to biopsy or a prolonged MRI examination with unnecessary acquisitions. By following recommendations from *Radiology Compliance Manager* [23], we billed patients for a limited MRI of the abdomen without contrast agent, reducing the overall cost by approximately 67%.

Our data found a total mean table time of 6–7 minutes. Although this time is very short, we believe that it likely represents an overestimate of our current mean table time. These data included the first few dozen examinations performed clinically at our institution while our

technologists were still familiarizing themselves with the protocol. Although nearly 60% of these examinations were performed in 6 minutes or less, for undocumented reasons, 11 examinations required 10 or more minutes of table time. We anticipate that mean table time will continue to decline as use of the rapid fat and iron protocol increases and our technologists become more familiar with the protocol. On the basis of our data, we currently schedule a 15-minute appointment to complete this examination, which is the shortest examination appointment time available in our electronic medical record scheduling software.

We have shown the successful use of this protocol in patients of all ages, with a range of 7–89 years documented in our initial experience. In fact, the information gained from the rapid fat and iron protocol has already been shown to be of prognostic value in adolescents [26]. We were able to perform this protocol without the need for sedation in any patients, making it an especially attractive option for children and adults who may have difficulty tolerating a lengthy MRI examination. Furthermore, our group and others have recently developed and validated an alternative CSE-MRI method for acquiring this examination, which is robust during free breathing and eliminates the need for patients to hold their breath [27, 28]. The ability to perform the rapid fat and iron protocol during free breathing combined with an overall reduced examination time and reduced cost would only increase the value to patients and referring providers.

By billing this examination as a limited abdominal MRI without contrast agent, we are able to offer the rapid fat and iron protocol at approximately one-third the price of a routine abdominal MRI with and without contrast agent. This is particularly important in an era where health care usage and costs are subject to increased scrutiny, by both patients individually and the public at large. For patients for whom the only relevant clinical question is the presence and degree of hepatic steatosis or iron overload, the ability to offer a protocol that answers the specific clinical question without superfluous sequences is critical. For radiologists, interpreting the examination is relatively straightforward, requiring placement of ROIs over the liver and reporting of the corresponding PDFF and R2* values [29]. When billed as an MRI of the abdomen without contrast agent and a limited modifier, the cost of the rapid fat and iron MRI examination is less than that of an abdominal CT without contrast agent and only \$20 and \$50 more expensive than complete and limited abdominal ultrasound, respectively. The quantitative MRI study provides quantitative information on the presence and severity of both liver fat and iron content, neither of which can be assessed as accurately with CT or ultrasound. However, recent studies have suggested a linear correlation between liver MRI PDFF and CT attenuation (in Hounsfield units) [30, 31] and have found reasonable sensitivity for the detection of hereditary hemochromatosis with unenhanced CT [32]. Given the high overall use of abdominal CT in the United States [33, 34], findings suggestive of either fatty liver or elevated liver iron at CT could represent an important entry point into potential MRI-based surveillance.

Our initial experience indicates that we still have considerable room for growth in use. In this initial cohort, abnormally elevated liver PDFF was detected in nearly all patients imaged for hepatic steatosis, and abnormally elevated R2* was detected in nearly half of patients imaged for iron overload. These high rates of positive findings suggest a very high level of

clinical suspicion or strong clinical evidence of abnormality in this population and strongly suggest underutilization of this protocol during this period. A reasonable argument can be made that the rapid fat and iron protocol offers the greatest amount of promise in patients for whom the clinical scenario is perhaps more ambiguous, and we foresee increased usage of this examination in the future in a wider array of patients. We have already seen this protocol successfully used for treatment monitoring for several patients who underwent multiple examinations to monitor hepatic steatosis. We were able to show the treatment progress in these patients and saw a mean decrease in PDFF by approximately 4% during the follow-up interval. Furthermore, patients with iron overload often require treatment monitoring, and, consequently, focused MRI may be a useful option for patients with hemochromatosis being treated with phlebotomy or patients with transfusional hemosiderosis undergoing chelator therapy.

Conclusion

In conclusion, we have successfully developed and implemented a focused CSE-MRI protocol that can assess hepatic fat and iron content in as little as 2–3 minutes of table time. Our initial clinical experience has also shown the feasibility of this protocol for evaluation of patients ranging from pediatric to geriatric at a relatively low cost, with clinically significant disease detected in a large fraction of patients. Furthermore, as our staff becomes increasingly comfortable performing and interpreting the examination and awareness among our referring providers increases, we are optimistic that usage of the rapid fat and iron protocol will increase. By implementing this focused MRI protocol, we aim to provide a rapid, inexpensive, and noninvasive tool for accurate and precise detection and treatment monitoring of hepatic steatosis and hepatic iron overload and to add additional value for our patients and referring providers.

Acknowledgments

Supported in part by grants R01-DK083380, R01-DK088925, R01-DK100651, R01-DK117354, and K24-DK102595 from the National Institutes of Health and by research support from GE Healthcare to the University of Wisconsin.

B. D. Pooler is a consultant for InnoVenn. D. Hernando is a founder of Calimetrix, LLC. S. B. Reeder is a Romnes Faculty Fellow; has received an award provided by the University of Wisconsin-Madison Office of the Vice Chancellor for Research and Graduate Education with funding from the Wisconsin Alumni Research Foundation; has ownership interests in Collectar Biosciences, Reveal Pharmaceuticals, and Elucent Medical; and is a founder of Calimetrix, LLC.

References

1. Ahmed A, Wong RJ, Harrison SA. Nonalcoholic fatty liver disease review: diagnosis, treatment, and outcomes. *Clin Gastroenterol Hepatol* 2015; 13:2062–2070 [PubMed: 26226097]
2. Schwimmer JB, Deutsch R, Kahen T, Lavine JE, Stanley C, Behling C. Prevalence of fatty liver in children and adolescents. *Pediatrics* 2006; 118:1388–1393 [PubMed: 17015527]
3. Gramlich T, Kleiner DE, McCullough AJ, Matteoni CA, Boparai N, Younossi ZM. Pathologic features associated with fibrosis in nonalcoholic fatty liver disease. *Hum Pathol* 2004; 35:196–199 [PubMed: 14991537]
4. Matteoni CA, Younossi ZM, Gramlich T, Boparai N, Liu YC, McCullough AJ. Nonalcoholic fatty liver disease: a spectrum of clinical and pathological severity. *Gastroenterology* 1999; 116:1413–1419 [PubMed: 10348825]

5. Adams LA, Lymp JF, St Sauver J, et al. The natural history of nonalcoholic fatty liver disease: a population-based cohort study. *Gastroenterology* 2005; 129:113–121 [PubMed: 16012941]
6. Pais R, Redheuil A, Cluzel P, Ratzu V, Giral P. Relationship between fatty liver, specific and multiple-site atherosclerosis and 10-year Framingham Score. *Hepatology* 2018 8 19 [Epub ahead of print]
7. Heron M Deaths: leading causes for 2014. *Natl Vital Stat Rep* 2016; 65:1–96
8. Morrison AE, Zaccardi F, Khunti K, Davies MJ. Causality between non-alcoholic fatty liver disease and risk of cardiovascular disease and type 2 diabetes: a meta-analysis with bias analysis. *Liver Int* 2018 10 25 [Epub ahead of print]
9. George DK, Goldwurm S, MacDonald GA, et al. Increased hepatic iron concentration in nonalcoholic steatohepatitis is associated with increased fibrosis. *Gastroenterology* 1998; 114:311–318 [PubMed: 9453491]
10. Niederau C, Fischer R, Pürschel A, Stremmel W, Häussinger D, Strohmeyer G. Long-term survival in patients with hereditary hemochromatosis. *Gastroenterology* 1996; 110:1107–1119 [PubMed: 8613000]
11. Papanikolaou G, Pantopoulos K. Iron metabolism and toxicity. *Toxicol Appl Pharmacol* 2005; 202:199–211 [PubMed: 15629195]
12. Kleiner DE, Brunt EM, Van Natta M, et al.; Nonalcoholic Steatohepatitis Clinical Research Network. Design and validation of a histological scoring system for nonalcoholic fatty liver disease. *Hepatology* 2005; 41:1313–1321 [PubMed: 15915461]
13. Bravo AA, Sheth SG, Chopra S. Liver biopsy. *N Engl J Med* 2001; 344:495–500 [PubMed: 11172192]
14. Reeder SB, Cruite I, Hamilton G, Sirlin CB. Quantitative assessment of liver fat with magnetic resonance imaging and spectroscopy. *J Magn Reson Imaging* 2011; 34:729–749 [PubMed: 22025886]
15. Hernando D, Levin YS, Sirlin CB, Reeder SB. Quantification of liver iron with MRI: state of the art and remaining challenges. *J Magn Reson Imaging* 2014; 40:1003–1021 [PubMed: 24585403]
16. Bannas P, Kramer H, Hernando D, et al. Quantitative magnetic resonance imaging of hepatic steatosis: validation in ex vivo human livers. *Hepatology* 2015; 62:1444–1455 [PubMed: 26224591]
17. Idilman IS, Aniktar H, Idilman R, et al. Hepatic steatosis: quantification by proton density fat fraction with MR imaging versus liver biopsy. *Radiology* 2013; 267:767–775 [PubMed: 23382293]
18. Reeder SB, Hu HH, Sirlin CB. Proton density fatfraction: a standardized MR-based biomarker of tissue fat concentration. *J Magn Reson Imaging* 2012; 36:1011–1014 [PubMed: 22777847]
19. Wood JC, Enriquez C, Ghugre N, et al. MRI R2 and R2* mapping accurately estimates hepatic iron concentration in transfusion-dependent thalassemia and sickle cell disease patients. *Blood* 2005; 106:1460–1465 [PubMed: 15860670]
20. Szczepaniak LS, Nurenberg P, Leonard D, et al. Magnetic resonance spectroscopy to measure hepatic triglyceride content: prevalence of hepatic steatosis in the general population. *Am J Physiol Endocrinol Metab* 2005; 288:E462–E468 [PubMed: 15339742]
21. Maeda JLK, Nelson L. How do the hospital prices paid by Medicare Advantage plans and commercial plans compare with Medicare fee-for-service prices? *Inquiry* 2018; 55:46958018779654
22. Centers for Medicare & Medicaid Services website. Physician fee schedule look-up tool. www.cms.gov/Medicare/Medicare-Fee-for-Service-Payment/PFSLookup/index.html. Published August 3, 2017 Accessed September 25, 2018
23. [No authors.] Questions and answers: focus on radiology services. *Radiology Compliance Manager* 2016; 19:1–4
24. Cho CS, Curran S, Schwartz LH, et al. Preoperative radiographic assessment of hepatic steatosis with histologic correlation. *J Am Coll Surg* 2008; 206:480–488 [PubMed: 18308219]
25. Schwenzer NF, Springer F, Schraml C, Stefan N, Machann J, Schick F. Non-invasive assessment and quantification of liver steatosis by ultrasound, computed tomography and magnetic resonance. *J Hepatol* 2009; 51:433–445 [PubMed: 19604596]

26. Rehm JL, Connor EL, Wolfgram PM, Eickhoff JC, Reeder SB, Allen DB. Predicting hepatic steatosis in a racially and ethnically diverse cohort of adolescent girls. *J Pediatr* 2014; 165:319e1–325.e1 [PubMed: 24857521]
27. Pooler BD, Hernando D, Ruby JA, Ishii H, Shimaka-wa A, Reeder SB. Validation of a motion-robust 2D sequential technique for quantification of hepatic proton density fat fraction during free breathing. *J Magn Reson Imaging* 2018; 48:1578–1585 [PubMed: 29665193]
28. Motosugi U, Hernando D, Bannas P, et al. Quantification of liver fat with respiratory-gated quantitative chemical shift encoded MRI. *J Magn Reson Imaging* 2015; 42:1241–1248 [PubMed: 25828696]
29. Campo CA, Hernando D, Schubert T, Bookwalter CA, Pay AJV, Reeder SB. Standardized approach for ROI-based measurements of proton density fat fraction and R2* in the liver. *AJR* 2017; 209:592–603 [PubMed: 28705058]
30. Kramer H, Pickhardt PJ, Kliever MA, et al. Accuracy of liver fat quantification with advanced CT, MRI, and ultrasound techniques: prospective comparison with MR spectroscopy. *AJR* 2017; 208:92–100 [PubMed: 27726414]
31. Pickhardt PJ, Graffy PM, Reeder SB, Hernando D, Li K. Quantification of liver fat content with unenhanced MDCT: phantom and clinical correlation with MRI proton density fat fraction. *AJR* 2018; 211:[web]W151–W157 [PubMed: 30016142]
32. Lawrence EM, Pooler BD, Pickhardt PJ. Opportunistic screening for hereditary hemochromatosis with unenhanced CT: determination of an optimal liver attenuation threshold. *AJR* 2018; 211:1206–1211 [PubMed: 30300001]
33. Moreno CC, Hemingway J, Johnson AC, Hughes DR, Mittal PK, Duszak R Jr. Changing abdominal imaging utilization patterns: perspectives from medicare beneficiaries over two decades. *J Am Coll Radiol* 2016; 13:894–903 [PubMed: 27084072]
34. Power SP, Moloney F, Twomey M, James K, O'Connor OJ, Maher MM. Computed tomography and patient risk: facts, perceptions and uncertainties. *World J Radiol* 2016; 8:902–915 [PubMed: 28070242]

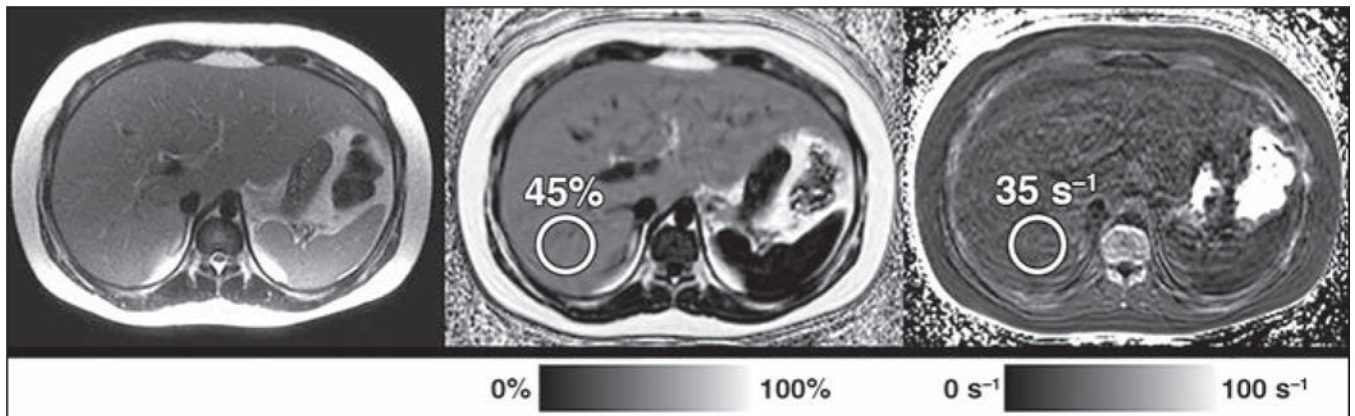


Fig. 1-
10-year-old boy with elevated aminotransferase level. Rapid fat and iron chemical shift–encoded MRI protocol shows severe hepatic steatosis. Proton density fat fraction (PDFF) map (*middle*) shows that patient has elevated PDFF of 45% (normal, < 5%) measured in posterior right hepatic lobe. R2* map (*right*) shows that R2* is normal at 35 s^{-1} (normal, < 60 s^{-1} at 1.5 T). Axial T2-weighted single-shot fast spin-echo MR image (*left*) is shown for reference. Interpretation of images is simple and straightforward, requiring only placement of ROIs (*circles*) over liver and reporting corresponding value.

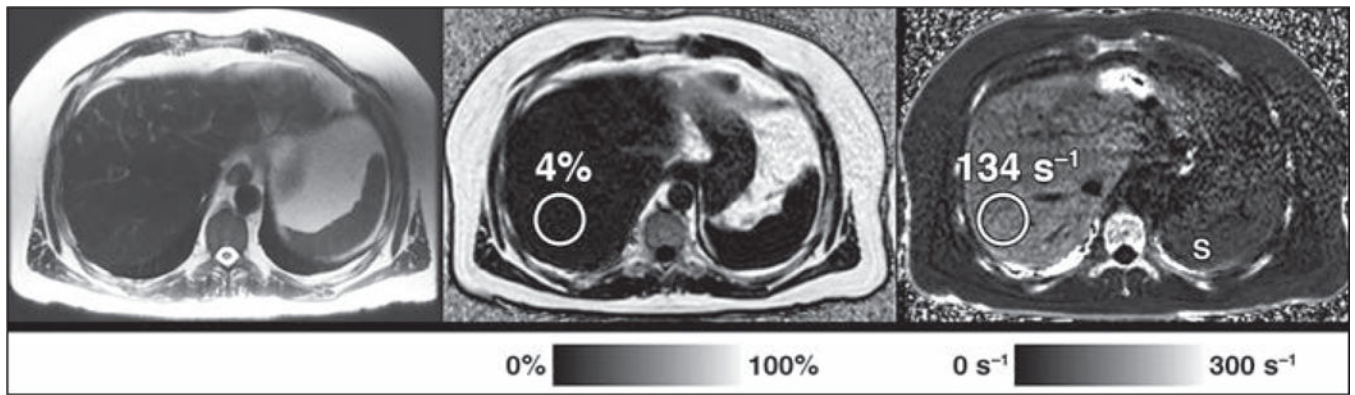


Fig. 2-

49-year-old man with hereditary hemochromatosis. Rapid fat and iron chemical shift-encoded MRI protocol shows mild hepatic iron overload. R2* map (*right*) shows elevated R2* of 134 s^{-1} (normal, $< 120 \text{ s}^{-1}$ at 3 T) as measured in posterior right hepatic lobe. Proton density fat fraction (PDFF) map (*middle*) shows that PDFF is normal at 4% (normal, $< 5\%$). Axial T2-weighted single-shot fast spin-echo MR image (*left*) is shown for reference. Note cirrhotic configuration of liver and T2 hypointensity of liver parenchyma due to increased iron, as well as lower R2* signal in spleen (S, *right*), indicative of normal iron content, which is typical pattern of iron overload in patients with hemochromatosis. Circles denote ROIs.

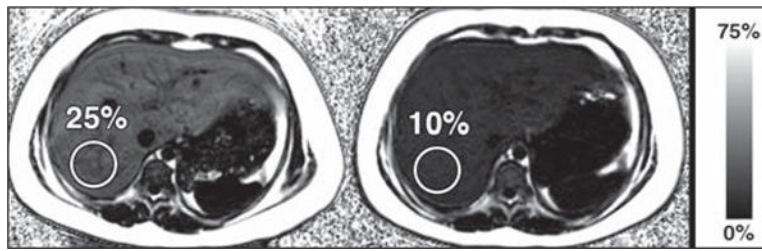


Fig. 3-
9-year-old girl with suspected hepatic steatosis. Rapid fat and iron chemical shift-encoded MRI protocol shows interval improvement in liver proton density fat fraction (PDFF) at follow-up. PDFF maps from initial examination (*left*) and follow-up examination performed 189 days later (*right*) show interval decrease in liver PDFF from 25% to 10% (normal liver PDFF, < 5%), thus showing substantial interval improvement in hepatic steatosis. Circles denote ROIs.

TABLE 1:
Scan Parameters for Chemical Shift-Encoded MRI Acquisitions at 1.5 and 3 T

Parameter	1.5 T	3 T
FOV (cm)	40 × 32	40 × 40
Slice thickness (mm)	8	8
Matrix	224 × 160	224 × 160
TR (ms)	13.8	7.5
TE1/ TE (ms)	0.9/0.9	0.9/2.0
Flip angle (°)	5	3
No. of echoes	6	6
Echoes per TR	6	3
Receiver bandwidth (kHz)	± 125	± 83.3
Scan time (s)	18	20

Note—TE1 = time to first echo, TE = echo time spacing.

TABLE 2: Centers for Medicare & Medicaid Services (CMS) Physician Fee Schedule Payment Information

Characteristic	MRI Abdomen	MRI Abdomen	CT Abdomen	Ultrasound	Ultrasound
	Without Contrast Limited	With and Without Contrast	Without Contrast ^a	Abdomen Limited	Abdomen Complete
Current Procedural Terminology code	74181-52	74183	74150	76705	76700
Technical component (TC)					
TC RVUs	5.92	8.97	2.54	1.77	2.34
TC reimbursement (TC RVUs × CF)	\$213.12	\$322.92	\$91.44	\$63.72	\$84.24
Professional component (PC)					
PC RVUs	2.08	3.13	1.70	0.84	1.15
PC reimbursement (PC RVUs × CF)	\$74.88	\$112.68	\$61.20	\$30.24	\$41.40
Overall price (TC + PC)	\$288.00	\$435.60	\$152.64	\$93.96	\$125.64
Limited modifier (-52), if applicable	-\$144.00	NA	NA ^a	NA	NA
Overall CMS price	\$144.00	\$435.60	\$152.64 ^a	\$93.96	\$125.64

Note—Data were retrieved September 25, 2018 [22]. RVU = relative value unit, CF = conversion factor (\$35,9996/RVU as of September 25, 2018), NA = not applicable.

^a Depending on indication, CT of the abdomen without could optionally be performed as a limited study. Application of the (-52) modifier in this case would decrease the price by \$76.32 (50%) to an overall CMS price of \$76.32.